ELSEVIER

Journal of Hazardous Materials B133 (2006) 233–242

Journal of Hazardous Materials

www.elsevier.com/locate/jhazmat

Equilibrium studies for trimethoprim adsorption on montmorillonite KSF

Zehra Bekçi, Yoldaş Seki, M. Kadir Yurdakoç *

Dokuz Eylül University, Faculty of Arts and Sciences, Department of Chemistry, 35160 Buca, İzmir, Turkey

Received 21 June 2005; received in revised form 5 October 2005; accepted 10 October 2005
Available online 28 November 2005

Abstract

In this study, the adsorption of trimethoprim (TMP) on montmorillonite KSF was studied under different conditions (pH, ionic strength, temperature). The results indicate that a pH value of 5.04 is optimum value for the adsorption of TMP on KSF. The adsorption kinetics was interpreted using pseudo-first-order kinetic model, pseudo-second-order kinetic model and intraparticle diffusion model. The pseudo-second-order model provides the best correlation with the experimental data of KSF adsorption. The adsorption data could be fitted with Freundlich, Langmuir and Dubinin-Radushkevich equation to find the characteristic parameters of each model. It was found that linear form of Langmuir isotherm seems to produce a better model than linear form of Freundlich equation. From the Langmuir and Freundlich equation, the adsorption capacity values raised as the solution temperature decreased. From DR isotherm, it was also determined that the type of adsorption can be considered as ion-exchange mechanism. Determination of the thermodynamic parameters ΔH^0, ΔS^0 and ΔG^0 showed that adsorption was spontaneous and exothermic in nature. It was also added that adsorption of TMP by KSF may involve physical adsorption.

Keywords: Trimetophrim; Adsorption; Montmorillonite; Adsorption kinetics; FT-IR

1. Introduction

Human and veterinary drugs are continually being released in the environment mainly as a result of manufacturing processes, disposal of unused or expired products, and excreta [1]. Antibiotics have wide range of uses in both human and veterinary medicine. In the livestock industry, the use of antibiotics as growth promoters as well as therapeutic agents is very common [2]. As a result, it is possible to determine antibiotics in the environment. Antibiotics have been determined in diverse environmental samples, e.g. wastewater [3], ground and river water [4,5], hospital wastewater [6], sludge [7], soil and manure [8,9]. For that reason, antibiotics released into the environment are of concern for the following reasons; (i) contamination of raw, treated and recycled water used for drinking, irrigation and recreation; (ii) potential to accelerate wide spread bacterial resistance to antibiotic; (iii) negative effect on important ecosystem bacteria (through death or inhibition) [10]. Their continual input into the environment may lead to a high, long-term concentration and promote unnoticed adverse effects on aquatic and terrestrial organisms. Effect can accumulate so slowly that changes remain undetected until they become irreversible [1].

Trimethoprim (TMP) is among the most important antibacterial agents (synthetic antibiotics) used in human and veterinary medicine worldwide acting as an inhibitor in the chemotherapy treatment due to its antifolate effect by interaction with dihydroflate coenzymes [11,12]. In respect of many articles, TMP was detected at 0.6–7.6 $\mu g\,L^{-1}$ level in hospital sewage water in Sweden [13], at 0.12 and 0.16 $\mu g\,L^{-1}$ levels in wastewater effluents from East Aurora and Holland, respectively [2], and 12.4 mg/kg level in manure and soil in a German farming area [14], and at 40–705 $ng\,L^{-1}$ in two municipal wastewater treatment plants in USA [15], and 0.013–0.15 $\mu g\,L^{-1}$ in US streams [5]. Additionally, a study made in Australia showed that TMP was detected in effluent entering receiving waters and detectable at 50 m from the site of discharge, and also in one bacterium (*E. coli*), resistance was observed to TMP [10]. Trimethoprim, 2,4-diamino-5-(3,4,5-trimethoxybenzyl)-pyrimidine is shown in Fig. 1.

It is impossible and impractical to halt usage of antimicrobial agents within our environments, though management of their overuse and disposal within catchments is likely to be an environmental management agenda in the near future [10].

* Corresponding author. Tel.: +90 232 4128695; fax: +90 232 4534188.
E-mail address: k.yurdakoc@deu.edu.tr (M.K. Yurdakoç).

0304-3894/$ – see front matter © 2005 Elsevier B.V. All rights reserved.
doi:10.1016/j.jhazmat.2005.10.029

Nomenclature

C_e	equilibrium concentration (mmol/L)
C_s	the amount of sorbed (mmol/g)
C_m	monolayer coverage (mmol g^{-1})
L	a constant (Langmuir)
K_f	relative adsorption capacity (mmol/g)
n_f	a constant (Freundlich)
X_m	the adsorption capacity (mol/g)
k	a constant (Dubinin-Radushkevich)
R	regression coefficient
E	the mean-free energy change of adsorption (kJ mol^{-1})
ΔG^0	standard-free energy change (kJ mol^{-1})
ΔH^0	standard enthalpy change (kJ mol^{-1})
ΔS^0	standard entropy change (kJ mol^{-1} K^{-1})
K_c	equilibrium constant
R	gas constant (J mol^{-1} K^{-1})
T	temperature (K)

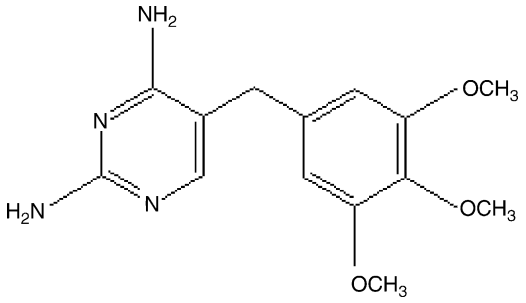

Fig. 1. Chemical structure of TMP.

To overcome destructive impacts of antibiotics released into the environment, it is very significant to design and develop a system to remove pharmaceuticals present in wastewater treatment plants. For this purpose, adsorption is appropriate process that is widely used in the removal of contaminants (e.g. pesticides) from wastewater. In view of the above fact that clays have high specific surface areas, high adsorption capacity, mechanical stability and variety of surface and structural properties, they are used as adsorbents for removing pollutants. This work reports the adsorption of trimethoprim onto montmorillonite KSF from aqueous solution as function of pH, temperature and ionic strength. Adsorption capacity of KSF for trimethoprim has been determined by using some common adsorption equilibrium models. In order to understand the adsorption process, kinetic and thermodynamic parameters obtained have also been evaluated at different temperatures.

2. Materials and methods

KSF supplied from Fluka Company was utilized for adsorption experiments as adsorbent. The properties of KSF were summarized in Table 1.

Table 1
Chemical composition of KSF montmorillonite

Component	%
SiO_2	55.0
Al_2O_3	18.0
Fe_2O_3	4.0
MgO	3.0
CaO	3.0
Na_2O	<0.5
K_2O	1.5
Sulphate	5.0
Ignition Loss	10.0

TMP was purchased from Merck and used without further purification. In the preparation of 10^{-3} M TMP stock solution, 0.02903 g TMP was weighed and dissolved in the mixture of 60 mL H_2O and 40 mL C_2H_5OH. Further solutions were freshly prepared from stock solution for each experimental study. For batch adsorption experiments, 0.1 g of KSF was added into 25 mL of TMP solution. The experiments have been made in duplicates. The pH of drug solution was adjusted with NaOH and HCl solutions using a pH meter. The solutions were shaken at 150 rpm in a temperature-controlled shaking water bath (Memmert) for 7 h to reach equilibrium under experimental conditions. After 7 h, the samples were taken and centrifuged at 5000 rpm for 15 min. The concentration of drug in resultant solution was determined using Shimadzu UV–vis 1601 model spectrophotometer at $\lambda_{max} = 271$ nm. The amount of TMP adsorbed on KSF montmorillonite was calculated by difference of initial concentration and the equilibrium concentration of TMP. The same procedures were performed at solution temperatures of 296, 311 and 323 K to find thermodynamic parameters. The ionic strengths were adjusted to 0.10, 0.05 and 0.01 using 1 M NaCl solutions. Some additional experiments were also carried out at various time intervals to determine kinetic parameters.

2.1. FT-IR measurements

TMP, KSF and TMP-loaded KSF were brought to constant weight in a drying oven at 50 °C for 24 h. The samples were kept in the desiccators. Fine KBr powder (100 mg) was dried at 110 °C and mixed with 1 mg of sample. For pellets obtained, the infrared spectra in the range 4000–400 cm^{-1} were recorded on a Perkin-Elmer FT-IR spectrophotometer (Spectrum BX-II).

2.2. SEM measurements

Scanning electron microscopy, SEM was carried out in a Jeol JSM 60 SEM attached an X-ray energy-dispersive spectrometer, EDS. The surface morphologies of KSF, TMP-loaded KSF were studied using a scanning electron microscope at an accelerating voltage of 20 kV. The samples that were used were dried and coated with gold before scanning. For SEM, photographs were taken at different magnifications (between 1000× and 5000×).

3. Result and discussion

3.1. Adsorption isotherms

The adsorption isotherm of TMP onto montmorillonite KSF was determined by plotting the amount of TMP adsorbed by KSF (C_s, mmol g^{-1}) versus the equilibrium concentration of TMP (C_e, mmol L^{-1}). The adsorption isotherms of TMP from aqueous solution onto KSF at different temperatures with initial pH 3.0 and without any salt addition are shown in Fig. 2. In terms of the slope of initial portion of the curves, the shapes of these isotherms correspond to L-type according to the Giles classification [16]. The L curve indicates that there is no strong competition between solvent molecules and adsorbate for sorption sites on the surface and KSF has a medium affinity for the TMP molecules.

In order to optimize the design of an adsorption system to remove the drug from the wastewater treatment plants, it is very significant to establish the most appropriate correlation for the equilibrium curves.

Three common adsorption equilibrium models (Langmuir, Freundlich, and Dubinin-Radushkevich (DR)) were used to describe the equilibrium between adsorbed TMP onto KSF (C_s) and TMP in solution (C_e) at constant temperatures.

3.1.1. Langmuir isotherm

The Langmuir isotherm theory assumes monolayer coverage of adsorbate over a homogeneous adsorbent surface [17]. In order to obtain sorption capacity of TMP on montmorillonite KSF, linear form of Langmuir equation was applied:

$$\frac{C_e}{C_s} = \frac{1}{LC_m} + \frac{C_e}{C_m} \quad (1)$$

where C_s is the solid phase concentration (mmol g^{-1}), C_e, the liquid phase concentration of adsorbate (mmol L^{-1}) at equilibrium, C_m, the maximum adsorption capacity (monolayer capacity of the adsorbent (mmol g^{-1}) and L is the Langmuir constant regarding the adsorption energy.

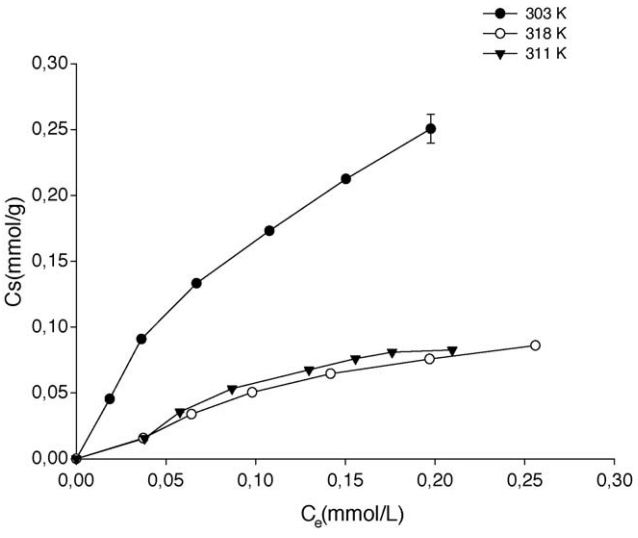

Fig. 2. Adsorption isotherms of TMP on KSF at different temperatures.

Table 2
The sorption parameters of Langmuir equation for TMP onto KSF at different temperatures

Temperature (K)	R^2	C_m (mmol g^{-1})	L (g dm^{-3})	R_L
303	0.9920	0.4461	5.8380	0.4613
311	0.9790	0.1686	4.1665	0.5455
318	0.9864	0.1400	7.2910	0.3138

C_m, maximum adsorption capacity; L, Langmuir constant; R ($p < 0.002$).

The Langmuir equation is applicable to homogenous sorption where the sorption of each molecule has equal sorption activation energy [18].

The sorption parameters of TMP adsorption onto KSF corresponding to Langmuir equation were summarized in Table 2. From Table 2, it is easily understood that maximum adsorption capacities of adsorbent decrease by increasing temperature.

To determine if the adsorption process is favorable or unfavorable, for the Langmuir type adsorption process, the isotherm shape can be classified by a term "R_L", a dimensionless constant separation factor, which is defined as below [19]:

$$R_L = \frac{1}{(1 + LC_0)} \quad (2)$$

where R_L is a dimensionless separation factor, C_0, the initial TMP concentration (mmol L^{-1}) and L is Langmuir constant (L $mmol^{-1}$).

The shapes of the isotherms for $0 < R_L < 1$, $R_L > 1$, $R_L = 1$ and $R_L = 0$ are favorable, unfavorable, linear and irreversible, respectively [19]. The values of R_L at different temperatures are reported in Table 2. The R_L values are between 0 and 1. Therefore, favorable adsorption of TMP was occurred.

3.1.2. Freundlich isotherm

The empirical Freundlich expression is an exponential equation and therefore, assumes that as the adsorbate concentration increases so too does the concentration of adsorbate on the adsorbent surface. Theoretically, using this expression, an infinite amount of adsorption can occur [20]:

$$C_s = K_f C_e^{n_f} \quad (3)$$

where C_s is the equilibrium drug concentration on adsorbent (mmol g^{-1}), C_e, the equilibrium drug concentration in solution (mmol L^{-1}), and K_f and n_f are the indicators of adsorption capacity and heterogeneity factor, respectively [18,21].

To determine the constants K_f and n_f, the linear form of Freundlich equation (Eq. (4)) is used:

$$\ln C_s = \ln K_f + n_f \ln C_e \quad (4)$$

By plotting $\ln C_s$ versus $\ln C_e$ for the adsorption of TMP at 303, 311 and 318 K onto montmorillonite KSF were utilized to obtain the intercept value of K_f and the slope value of n_f.

Freundlich constants were shown in Table 3. As seen apparently in Table 3, K_f values decrease by increasing temperature. This result indicates that TMP is more adsorbed at 303 K than

Table 3
The sorption parameters of Freundlich equation for adsorption of TMP onto KSF at different temperatures

Temperature (K)	R^2	K_f (mmol g^{-1})	n_f
303	0.983	0.824	0.700
311	0.950	0.319	0.861
318	0.961	0.232	0.628

K_f, relative adsorption capacity; n_f, adsorption intensity; R ($p < 0.002$).

Table 4
The sorption parameters of DR equation for TMP on KSF at different temperatures

Temperature (K)	R^2	X_m (mol g^{-1})	β (mol^2 kJ^{-2})	E (kJ mol^{-1})
303	0.976	0.00250	0.00513	9.872
311	0.962	0.00241	0.00705	8.422
318	0.971	0.00109	0.00503	9.970

X_m, adsorption capacity; k, a constant related to adsorption energy; E, free energy; R ($p < 0.09$).

311 and 318 K. As can be seen from Tables 2 and 3, Langmuir adsorption isotherm gave a better fit than the Freundlich model based on the correlation coefficients (R^2) value.

From Table 3, it is seen that the values of n_f are smaller than 1, reflecting a favorable adsorption. That the adsorption is favorable is also deduced from the dimensionless separation factors.

3.1.3. Dubinin-Radushkevich (DR) isotherm

By using Langmuir and Freundlich isotherms, the information regarding the adsorption type is not obtained. For finding out the adsorption type, the equilibrium data is applied to following linear form of DR isotherm:

$$\ln C_s = \ln X_m - \beta\varepsilon^2 \quad (5)$$

where C_s is the amount of ions sorbed onto the adsorbent (mol g^{-1}), X_m represents maximum adsorption capacity of the sorbent (mol g^{-1}), β, a constant related to sorption energy (mol^2 kJ^{-2}) and ε is the Polanyi sorption potential, the amount of energy required to pull a sorbed molecule from its sorption site to infinity which is equal to:

$$\varepsilon = RT \ln\left(1 + \frac{1}{C_e}\right) \quad (6)$$

where R is the gas constant in kJ mol^{-1} K^{-1}; T, the temperature in Kelvin and C_e is the equilibrium concentration in solution (mol L^{-1}).

By plotting $\ln C_s$ versus ε^2, the value of X_m is determined from the intercept and the value of β is derived from the slope.

The mean-free energy E was calculated using the following expression:

$$E = -(2\beta)^{-0.5} \quad (7)$$

The E values obtained in this study are in the range of 8–16 kJ mol^{-1}, designating for ion-exchange mechanism [22]. If sorption energy is smaller than 8 kJ mol^{-1}, adsorption type is physical adsorption due to weak van der Waals forces. DR isotherm parameters at 303, 311 and 318 K were summarized in Table 4. As can be seen from Table 4, E values are in the range of 8.42–9.97 kJ mol^{-1}. All of the E values indicate that sorption of TMP onto montmorillonite KSF can be explained by ion-exchange mechanism at 303, 311 and 318 K. These energy values are close to physical adsorption type. Besides, it is difficult to be certain that the type of adsorption is physical, since the E values obtained in this study are only slightly larger than 8 kJ mol^{-1}, X_m (maximum adsorption capacity of the sorbent) values were 2.504, 2.410 and 1.088 mmol g^{-1}, respectively. By increasing temperature, X_m values are decreasing.

3.2. Effect of pH on the adsorption process

The adsorptive treatment of drug-containing wastewater is pH-dependent. Therefore, the pH effect on the adsorption of TMP on KSF was studied at 299 K without any salt. For this study, solutions of concentration 0.4×10^{-3} M of the drug were prepared at different pH values. After the equilibrium was established, the absorbance and pH values were found out. In order to show the effects of pH on adsorption, the amount of TMP adsorbed by KSF (C_s, mmol g^{-1}) versus equilibrium pH was plotted. It is shown in Fig. 3. It is obvious that maximum adsorption at equilibrium was provided at pH 5.04.

Montmorillonite KSF is acid activated clay that has a pH value of 3.31 in an aqueous solution and TMP (Fig. 1) is a weak base with a pK_a value of 7.3. At low pH conditions, all of the TMP (T:) is in the protonated form:

$$TH^+ \leftrightarrow T : + H^+$$

Protonated form of the drug is strongly adsorbed to the negatively charged sites of KSF surface by cation-exchange process. For equilibrium pH below 5.04, a significantly high electrostatic attraction exists. As the pH of the system increased, a negatively charged surface site on the adsorbent did not favor the adsorption of neutral T: molecule. In other words, since the drug is

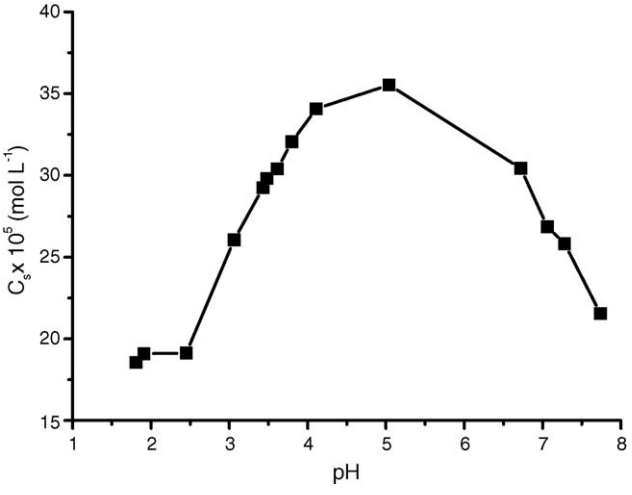

Fig. 3. pH effects on adsorption of TMP onto KSF.

Table 5
Isotherm parameters for TMP adsorption onto KSF at various temperatures

NaCl [M]	0.01	0.05	0.1
Langmuir model			
$R_L{}^2$	0.987	0.991	0.992
C_m (mmol g^{-1})	0.154	0.142	0.135
L (g L^{-1})	9.328	6.681	6.699
Freundlich model			
$R_F{}^2$	0.945	0.977	0.989
K_f (mmolg^{-1})	0.239	0.193	0.162
n_f	0.528	0.553	0.492
DR model			
$R_D{}^2$	0.957	0.985	0.993
X_m (mmolg^{-1})	0.836	0.749	0.560
E (kJ mol^{-1})	10.325	10.010	10.541

C_m, maximum adsorption capacity; L, Langmuir constant; R_L ($p<0.002$); K_f, relative adsorption capacity; n_f, adsorption intensity; R_F ($p<0.002$); X_m, adsorption capacity; k, a constant related to adsorption energy; E, free energy; R_D ($p<0.001$).

in neutral form at nearly pH 7.5, no significant ionic attraction was observed and the adsorption mechanism of TMP to KSF at basic conditions is physical one, and a weak one [23]. After the pH value of 5.04, the amount of TMP adsorbed is decreasing with the decrease of solution pH. This is due to fact that H^+ concentration is also decreasing with decrease of solution pH and a competition occurs between H^+ and protonated form of TMP molecules. As a result of this competition, the amount of TMP adsorbed at low pH is very low.

3.3. Effect of ionic strength on the adsorption process

Ionic strength is the most important variable in drug–clay interaction [24]. In the present study, ionic strength of the medium exhibited some effect on adsorption of TMP onto montmorillonite KSF at constant pH 4. The sorption parameters obtained from Langmuir, Freundlich and DR isotherm equations were summarized in Table 5. As was shown in Table 5, the amounts of TMP adsorbed on montmorillonite KSF were decreased with increased concentration of NaCl in medium. This result was similar to the investigation of Qtaitat [24] who studied the interaction of TMP–montmorillonite as a function of ionic strength. The amount of TMP adsorbed decreases with increase of ionic strength. The addition of salt causes competition between the protonated form of the drug molecules and Na^+ ions to negatively charged surface of the clay by cation-exchange mechanism in acidic condition. C_m (adsorption capacity for Langmuir isotherm), K_f (adsorption capacity for Freundlich isotherm) and X_m (maximum sorption capacity of the sorbent for DR isotherm) values are decreasing from 0.154 to 0.135 mmol g^{-1}; from 0.239 to 0.162 mmol g^{-1} and from 0.836 to 0.598 mmol g^{-1}, respectively.

3.4. Adsorption kinetics

The kinetics of sorption process of TMP onto KSF has also been explored. The time dependence curve of TMP adsorption was given in Fig. 4. Considering Fig. 4, contact time was fixed at 7 h in this study.

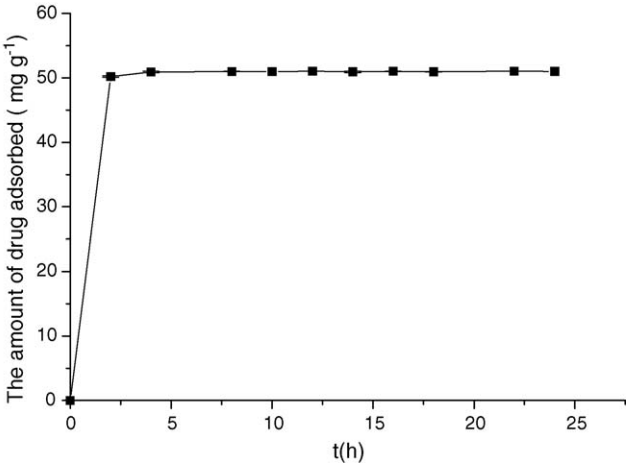

Fig. 4. Effect of contact time of TMP adsorption onto KSF.

It is seen that adsorption of TMP was rapid in the first stage, beyond which the rate of adsorption slowed down. Three models have been offered to reveal the adsorption kinetics of TMP onto KSF. One of them is pseudo-first-order kinetic model which is given by

$$\frac{1}{q_t} = \left(\frac{k_1}{q_1}\right)\left(\frac{1}{t}\right) + \frac{1}{q_1} \quad (8)$$

where q_t is the amount of TMP adsorbed at different times t (mg g^{-1}), k_1 is the pseudo-first-order rate constant for the adsorption process (min^{-1}). The value of q_1 is the maximum adsorption capacity (mg g^{-1}) [25]. A plot of $1/q_t$ versus $1/t$ should be a straight-line with a slope k_1/q_1 and intercept $1/q_1$. As was summarized in Table 6, the correlation coefficients (R^2) are between 0.845 and 0.980 for different temperatures.

Table 6
Kinetic parameters for TMP adsorption onto KSF at various temperatures

	296 K	311 K	323 K
Pseudo-first-order model			
$R_1{}^2$	0.960	0.845	0.980
k_1 (min^{-1})	18.024	13.172	16.993
q_1 (mg g^{-1})	27.427	24.085	22.472
Pseudo-second-order model			
$R_2{}^2$	0.998	0.999	1.000
k_2 (g mg^{-1} min^{-1})	0.004	0.006	0.011
q_2 (mg g^{-1})	26.406	23.697	21.716
Intraparticle diffusion model			
$R_p{}^2$	0.900	0.927	0.918
k_i (mg s$^{-1/2}$ g^{-1})	0.406	0.181	0.072
C	18.760	19.841	20.051

k_1, the pseudo-first-order rate constant; q_1, the maximum adsorption capacity for pseudo-first-order adsorption; k_2, pseudo-second-order rate constant; q_2 the maximum adsorption capacity for pseudo-second-order adsorption; k_i the intraparticle diffusion rate constant; C, a constant; R_1 ($p<0.03$), R_2 ($p<0.0001$), R_p ($p<0.009$).

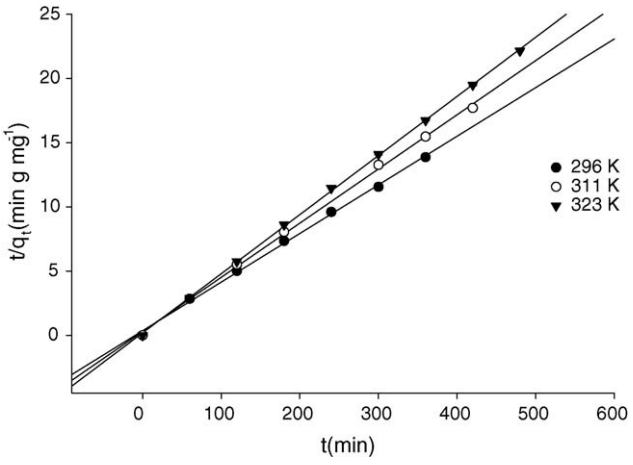

Fig. 5. Second-order kinetic plots for the adsorption of TMP onto KSF.

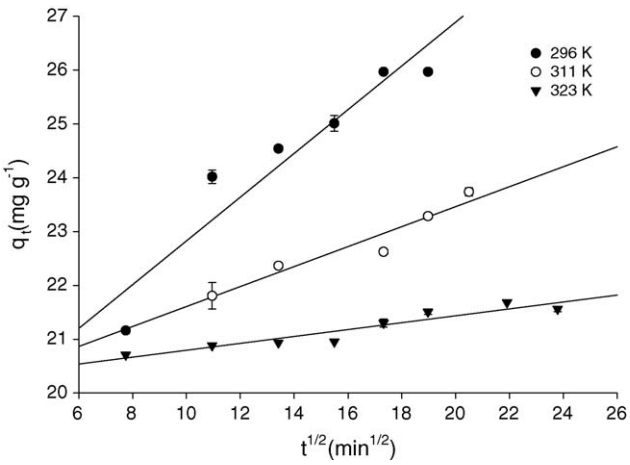

Fig. 6. Intraparticle mass transfer curve for adsorption of TMP onto KSF.

The other one is pseudo-second-order equation which can be shown with the following equation:

$$\frac{dq_t}{dt} = k_2(q_2 - q_t)^2 \quad (9)$$

where k_2 is the pseudo-second-order rate constant (mg g^{-1}) and q_2 is the maximum adsorption capacity for the second-order (g mg^{-1} min^{-1}).

After integration of Eq. (9), applying the initial conditions $q_t = 0$ at $t = 0$ and $q_t = q_t$ at $t = t$, equation can be written as

$$\frac{t}{q_t} = \left(\frac{1}{k_2^2}\right) + \frac{t}{q_2} \quad (10)$$

The straight-line plots of t/q_t versus t for the pseudo-second-order adsorption of TMP (Fig. 5) onto KSF have been applied to determine rate constants k_2 and q_2 at various temperatures. The results were given in Table 6.

The equations mentioned above, cannot identify the diffusion mechanism. Therefore, intraparticle diffusion model was applied to adsorption data. The intraparticle diffusion model which was used to describe the kinetics of TMP adsorption onto KSF is

$$q_t = k_i t^{1/2} + C \quad (11)$$

where k_i is the intraparticle diffusion rate constant (mg s$^{-1/2}$ g^{-1}) and C is the intercept. The value of C and k_i was obtained from the intercept and slope of the plot of q_t versus $t^{1/2}$ (Fig. 6). The values of the intercept give an idea about the thickness of boundary layer, i.e. the larger the intercept, the greater layer effect. Such types of plots may present multilinearity, implying that two or more steps occur [26]. A good conformity can identify the diffusion mechanism.

As was presented in Table 6, based on the R^2 values for TMP sorption, pseudo-second-order kinetic model appears to produce a better model in comparison with pseudo-first-order kinetic model. It was reached that q_2 values (maximum adsorption capacity for the second-order model) raised as the temperature of solution decreased from 323 to 296 K. This result is also consistent with the results that were estimated from pseudo-first-order kinetic model. However, k_2 values reduced when the temperature increased in the temperature range studied.

The maximum adsorption capacities for pseudo-second-order model were found to be 26.41, 23.70 and 21.72 mg g^{-1} for 296, 311 and 323 K, respectively. The decrease in the maximum adsorption capacity of TMP with temperature implies that a low temperature favors TMP adsorption onto KSF. This can be related to movements of TMP from the solid phase to the bulk phase with a rise in the temperature of the solution. It can be inferred that the type of adsorption can be considered as physical process. The intraparticle diffusion parameters for TMP adsorption were presented in Table 6. Based on R^2 values, the intraparticle diffusion model has a low-level compliance with our experimental data of TMP sorption onto KSF.

With an increase of the temperature from 296 to 323 K, the values of intraparticle diffusion rate constants decreased from 0.406 to 0.072 mg g^{-1} min$^{-1/2}$. It would be reached that, TMP molecules diffused in the pores of KSF. The rate of migration of TMP molecules to the pores of solid starts to slow down with an increase of the temperature. Therefore, intraparticle diffusion rate constant became lower in the temperature range of 296 and 323 K.

As can be seen from Table 6, correlation coefficients for the pseudo-second-order are greater than those of estimated for intraparticle diffusion. The pseudo-second-order equation predicts behavior over the whole range strongly supporting the validity and agrees with chemisorption being rate-controlling because it is basically based on the adsorption capacity [26,27].

The linear portions of the curves do not pass the origin, so it was proposed that in addition to intraparticle diffusion, other process may control the rate of adsorption. All of them may be operating simultaneously [28].

4. Thermodynamic parameters

In order to obtain activation energy of sorption process, Arrhenius equation was used in the following form:

$$\ln k_2 = \ln A - \frac{E_a}{RT} \quad (12)$$

Table 7
Thermodynamic parameters for TMP adsorption on KSF

T (K)	K_c	ΔG^0 (kJ mol^{-1})	ΔS^0 (kJ mol^{-1} K^{-1})	ΔH^0 (kJ mol^{-1})
296	2.338	−2.087	−41.145	−14.233
311	1.739	−1.428		
323	1.430	−0.960		

K_c is the equilibrium constant; ΔG^0, standard-free energy change; ΔH^0, standard enthalpy change; ΔS^0, standard entropy change.

where E_a is the activation energy of sorption, k_2, the pseudo-second-order rate constant, A, the Arrhenius constant, R, the gas constant (8.314 J mol^{-1} K^{-1}) and T is the solution temperature (K). The E_a value is obtained from the slope of Arrhenius plot of $\ln k_2$ against $1/T$. The importance of activation energy is that it is used to determine the type of adsorption (physical or chemical). The physisorption process usually has energies in the range of 5–40 kJ mol^{-1}, while higher activation energies (40–800 kJ mol^{-1}) suggest chemisorption [29]. In this study, E_a value was found to be 29.3 kJ mol^{-1}, indicating physisorption.

The Gibbs free energy for sorption process is computed using the following equations:

$$\Delta G^0 = -RT \ln K_c \quad (13)$$

$$K_c = \frac{C_s}{C_e} \quad (14)$$

where K_c is the equilibrium constant, C_e, the equilibrium concentration and C_s is the amount sorbed on solid at equilibrium. van't Hoff equation which was applied to obtain change in standard enthalpy (ΔH^0) and entropy (ΔS^0) can be given as below:

$$\ln K_c = -\frac{\Delta H_{ads}}{RT} + \frac{\Delta S}{R} \quad (15)$$

When $\ln K_c$ was plotted versus $1/T$, the values of ΔH^0 and ΔS^0 were estimated from the slope and intercept, respectively [23]. The results were presented in Table 7.

It is known that the absolute magnitude of the change in free energy for physisorption is between −20 and 0 kJ mol^{-1}; chemisorption has a range of −80 to −400 kJ mol^{-1} [28,30]. ΔG^0 values were calculated to be −2.07, −1.43 and −0.96 kJ mol^{-1} for 296, 311 and 323 K, respectively. This implies that adsorption of TMP onto KSF may occur as physically. This is also confirmed by the previous findings derived from Arrhenius equation. The negative values of ΔG^0 at various temperatures show the spontaneous nature of adsorption process. Moreover, it can be noted that the magnitude of ΔG^0 values is in the range of multilayer adsorption. Because, according to [28] the standard-free energy change for multilayer adsorption was more than −20 kJ mol^{-1} and less than zero.

The value of standard enthalpy change for TMP adsorption is −14.233 kJ mol^{-1} that is, interactions between TMP and KSF is exothermic in nature. Presumably, this supports multilayer adsorption which is mentioned above. In [27] report, when the value of ΔH^0 is lower than 40 kJ mol^{-1} the type of adsorption can be accepted as physical process. Since ΔH^0 value obtained in this study is lower than 40 kJ mol^{-1}, it would be claimed that physical adsorption occurs during adsorption. This can be explained by the fact that weak forces of attraction among TMP molecules may be observed. Since TMP molecules are not arranged in an ordered manner in solution phase, the standard entropy change for sorption process is negative. In other words, degrees of freedom of the adsorbed species are decreasing.

4.1. SEM analysis

The surface morphologies of clay and TMP-loaded clay which examined scanning electron microscopy (SEM) were presented in Figs. 7a and 8a, respectively. The chemical content of the clay and TMP-loaded clay were obtained using semiquantitative EDS data, which was given in Figs. 7b and 8b, respectively. In Fig. 7a, silicate layers with different sizes can be seen and disperse in various direction. It can be added that the distribution of silicate particles are heterogeneous. From EDS analysis of clay sample, it is determined that SiO_2 is the basic constituent of clay with the content of 60.109%. It can be deduced from the EDS analysis of TMP-loaded clay that constituent of SiO_2 was decreased to 42.063% after loading of TMP. However, the

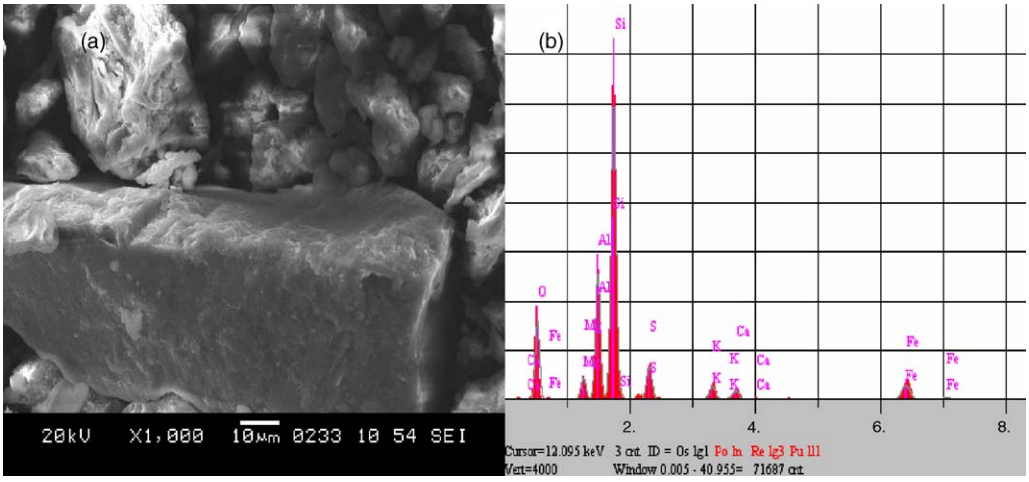

Fig. 7. SEM micrographs of (a) KSF (1000×); (b) EDS analysis of KSF.

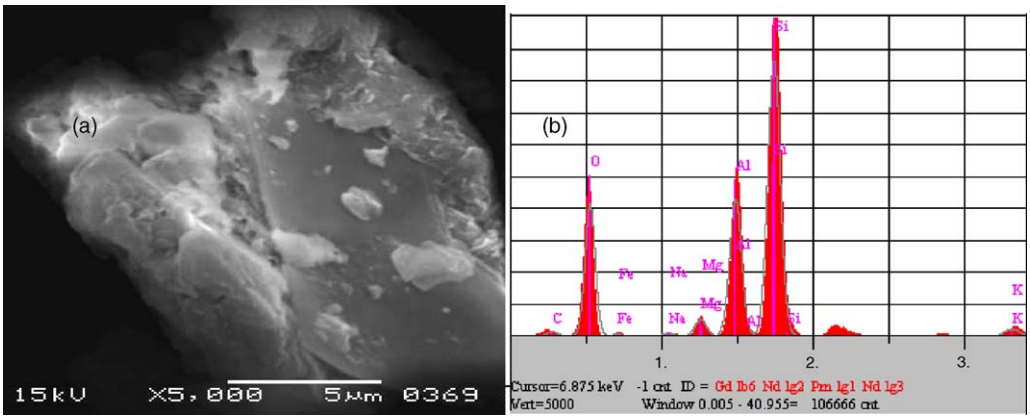

Fig. 8. SEM micrographs of (a) TMP-adsorbed KSF (5000×); (b) EDS analysis of TMP-adsorbed KSF.

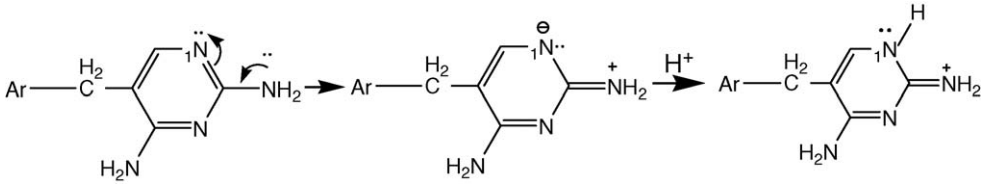

Scheme 1. Protonation of TMP.

content of carbon in drug-loaded clay was increased to 19.714% due to adsorption of TMP on clay.

4.2. FT-IR study of TMP adsorption

Fig. 9 displays the FT-IR spectra of TMP, TMP–KSF and KSF. As was illustrated in figure, the absorption band located at 1633 cm^{-1} in the spectrum of KSF is assigned to deformation mode of water. After adsorption of TMP, this band shifted to 1627 cm^{-1}. This small change may be indication of hydrogen bonding between water bonded to the clay and TMP. In the spectrum of TMP, the bands near 1593 and 1565 cm^{-1} can be evaluated as NH_2 deformation bands. Presumably, these bands cannot be seen easily due to combination of these bands with water deformation bands. In the spectrum of KSF, the bands detected at 529 and 479 cm^{-1} can be identified as Si–O–Al and Si–O–Si bending vibrations, respectively. After adsorption of TMP, small shifts were observed in these peaks. In the spectrum of KSF, a strong peak at 1045 cm^{-1} corresponds to Si–OH stretching vibration. When we compare two spectra (KSF and KSF–TMP), it is seen that, intensity of Si–OH stretching band is increased significantly. It may be due to difference in the environment. The band at 1686 cm^{-1} in the spectrum of TMP, was shifted to 1666 cm^{-1} in the spectrum of TMP–KSF which can be attributed to the stretching vibration of C=NH_2. According to [23], the most basic site at the heterocyclic ring of TMP is N_1 where protonation occurs. As can be seen from Scheme 1, C=NH_2 group which is the positively charged moiety of TMP interact with the negatively site of KSF as a consequence of ion-exchange between TMP and positively charged ions existing on clay surface. As a result of interaction, stretching vibration of C=NH_2 at 1686 cm^{-1} shifted to 1666 cm^{-1}. These results support the ion-exchange mechanism for TMP adsorption onto KSF, which is supported by DR isotherm.

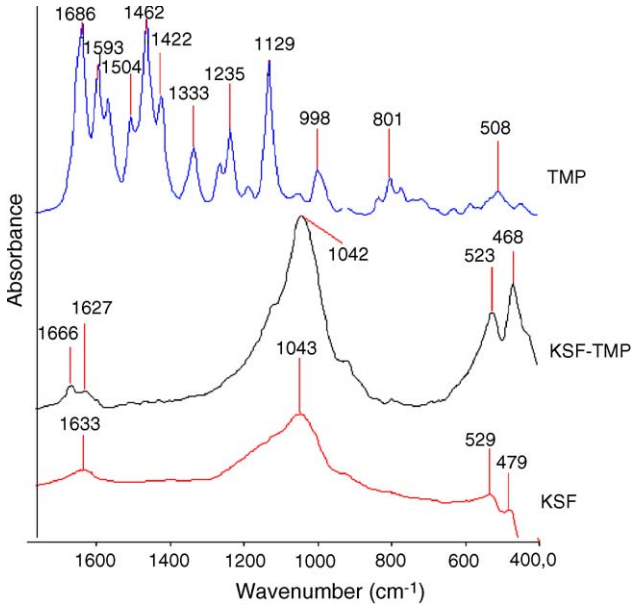

Fig. 9. FT-IR spectrum of KSF, KSF–TMP and TMP.

5. Conclusion

To get under control the release of drugs to environment, montmorillonite KSF has been suggested for removing drugs from wastewater and hospital sewage water. If releasing of drugs

to environment goes on in this way, antibiotics and resistant bacteria will increase in the local waterways and this will affect the biotic process because of transferring resistance genes from harmless bacteria to pathogenic bacteria and on to humans interacting with the aquatic environment. Additionally, it is forced to develop new antibiotics that have a long while and expensive preparing process.

Clay minerals including KSF are efficient and economic natural adsorbents of pollutants. The Langmuir, Freundlich and DR adsorption isotherms were used to obtain isotherm constants for evaluating the adsorption in various temperatures and ionic strengths. Langmuir adsorption isotherm gave a better fit than the Freundlich model based on the correlation coefficients (R^2) values. Adsorption of TMP which widely used in usual life of animals and humans is increased by decreasing temperature, which is inferred from adsorption isotherms and kinetic inputs. All E (sorption energy) values obtained from DR adsorption isotherm were between 8 and 16 kJ mol^{-1}, for that reason these E values indicate that sorption of TMP onto KSF can be explained by ion-exchange mechanism at 303, 311 and 318 K and energy values are close to physical adsorption type. The adsorptive removal of drug from aqueous solution is pH and ionic intensity dependent. The maximum adsorption at equilibrium was observed at pH 5.04. At lower pH, adsorption is high via the attraction between the negatively charged surface of clay and protonated form of the drug. The amounts of TMP adsorbed on KSF were decreased with increased concentration of NaCl in medium owing to the competition to negatively charged clay surface between the protonated form of TMP and Na^+ ions.

From kinetic models applied to experimental data, pseudo-second-order model was found to be best model. The fit of intraparticle diffusion was also investigated. It is determined that the compliance is poor. In terms of intraparticle diffusion model, the linear portions of the curves do not pass the origin, this indicates that the intraparticle diffusion is not the only rate-controlling step and adsorption mechanism of TMP onto KSF is complex. The activation energy of adsorption was determined as 29.3 kJ mol^{-1} indicating physisorption. Thermodynamic parameters; ΔH^0, ΔS^0 and ΔG^0 were estimated and these parameters show that occurred adsorption is exothermic, favorable and spontaneous, respectively. It can be concluded that the mechanism of adsorption is carried out with the combination of ion-exchange mechanism and physical adsorption.

Application of adsorption for the removal of TMP can be appropriate for the designing of wastewater treatment plants by using these kinetic parameters. It is impossible and unpractical to stop antibiotic disposal. For that reason, this study will give a route near future investigation relating to the removing drugs from the environment.

Acknowledgement

The Authors also thank to Murat Kuşoğlu (Dokuz Eylül University, Faculty of Engineering, Department of Metallurgical and Materials Engineering).

References

[1] M.S. Diaz-Cruz, M.J. Lopez de Alda, D. Barcelo, Environmental behavior and analysis of veterinary and human drugs in soils, sediments and sludge, Trends Anal. Chem. 22 (6) (2003) 340–351.
[2] A.L. Batt, D.S. Aga, Simultaneous analysis of multiple classes of Antibiotics by Ion Trap LC/MS/MS for assessing surface water and ground water contamination, Anal. Chem. 77 (2005) 2940–2947.
[3] R. Hirsch, T.A. Ternes, K. Haberer, A. Mehlich, F. Ballwanz, K.-L. Kratz, Determination of antibiotics in different water compartments via liquid chromatography electrospray tandem mass spectrometry, J. Chromatogr. A 815 (1998) 213–223.
[4] F. Sacher, F.T. Lange, H.J. Brauch, I. Blankenhorn, Pharmaceuticals in groundwaters: analytical methods and results of a monitoring program in Baden-Württemberg, Germany, J. Chromatogr. A 938 (2001) 199–210.
[5] D.W. Kolpin, E.T. Furlong, M.T. Meyer, E.M. Thurman, S.D. Zaugg, L.B. Barber, H.T. Buxton, Pharmaceuticals, hormones, and other organic wastewater contaminants in US streams, 1999–2000: a national reconnaissance, Environ. Sci. Technol. 36 (2002) 1202–1211.
[6] A. Hartmann, E.M. Golet, S. Gartiser, A.C. Alder, T. Koller, R.M. Widmer, Primary DNA damage but not mutagenicity correlates with ciprofloxacin concentrations in German hospital wastewaters, Primary Arch. Environ. Contam. Toxicol. 36 (1999) 115–119.
[7] E.M. Golet, A.C. Alder, A. Hartmann, T.A. Ternes, W. Giger, Trace determination of fluoroquinolone antibacterial agents in sewage sludge-treated soil using accelerated solvent extraction followed by solid phase extraction, Anal. Chem. 73 (2001) 3632–3638.
[8] Y. Haller, S.R. Muller, C.S. McArdell, A.C. Alder, M.J.F. Suter, Quantification of veterinary antibiotics (sulfonamides and trimethoprim) in animal manure by liquid chromatography–mass spectrometry, J. Chromatogr. A 952 (2002) 111–120.
[9] G. Hamscher, S. Sczesny, H. Hoper, H. Nau, Determination of persistent tetracycline residues in soil fertilized with liquid manure by high-performance liquid chromatography with electrospray ionization tandem mass spectrometry, Anal. Chem. 74 (2002) 1509–1518.
[10] S.D. Costanzo, J. Murby, J. Bates, Ecosystem response to antibiotics entering the aquatic environment, Mar. Pollut. Bull. 51 (2005) 218–223.
[11] K. Florey (Ed.), Analytical Profile of Drug Substances, 7, Academic Press, New York, 1978, p. 459.
[12] G.H. Hitchings, J.J. Burchall, Advances in Enzymology, 27, Wiley/Interscience, New York, 1965, p. 417.
[13] R. Lindberg, P.-A. Jarnheimer, B. Olsen, M. Johonsson, M. Tysklind, Determination of antibiotic substances in hospital sewage water using solid phase extraction and liquid chromatography/mass spectrometry and group analogue internal standards, Chemosphere 57 (2004) 1479–1488.
[14] X.-S. Miao, F. Bishay, M. Chen, C.D. Metcalfe, Occurrence antimicrobials in the final effluents of wastewater treatment plants in Canada, Environ. Sci. Technol. 38 (2004) 3533–3541.
[15] J.E. Renew, C.-H. Huang, Simultaneous determination of flurorquinolone, sulfonamide, and trimethoprim antibiotics in wastewater using tandem solid phase extraction and liquid chromatography–electrospray mass spectrometry, J. Chromatogr. A 1042 (2004) 113–121.
[16] C.H. Giles, T.H. McEvan, S.N. Nakhwa, D. Smith, Studies in adsorption. Part II. A system of classification of solution adsorption isotherms, J. Chem. Soc. 4 (1960) 3293–3973.
[17] I. Langmuir, Adsorption of gases on plane surfaces of glass, mica and platinum, J. Am. Chem. Soc. 40 (1918) 1361–1403.
[18] S.J. Allen, Q. Gan, R. Matthews, P.A. Johnson, Comparison of optimized isotherm models for basic dye adsorption by kudzu, Bioresource Technol. 88 (2003) 143–152.
[19] T.W. Weber, R.K. Chakkravorti, Pore and solid diffusion models for fixed bed adsorbers, Am. Inst. Chem. Eng. J. 20 (1974) 228–238.
[20] H. Freundlich, Adsorption in solution, Phys. Chem. 57 (1906) 384–410.
[21] Z. Aksu, E. Kabasakal, Batch adsorption of 2,4-dichlorophenoxy-acetic acid (2,4-D) from aqueous solution by granular activated carbon, Sep. Purif. Technol. 35 (2004) 223–240.

[22] U.R. Malik, S.M. Nasany, M.S. Subhani, Sorptive potential of sunflower stern for Cr(III) ions from aqueous solution and its kinetic and thermodynamic profile, Talanta 66 (2005) 166–173.
[23] D.R. Narine, R.D. Guy, Interactions of some large organic cations with bentonite in dilute aqueous systems, Clays Clay Miner. 29 (1981) 205–212.
[24] M.A. Qtaitat, Study of interaction of trimethoprim–montmorillonite by infrared spectroscopy, Spectrochim. Acta Part A 60 (2004) 673–678.
[25] M. Yurdakoc, Y. Seki, S. Karahan, K. Yurdakoc, Kinetic and thermodynamic studies of boron removal by Siral 5, Siral 40 and Siral 80, J. Colloid Interf. Sci. 286 (2005) 440–446.
[26] S. Karaca, A. Gürses, M. Ejder, M. Açıkyıldız, Kinetic modeling of liquid-phase adsorption of phosphate on dolomite, J. Colloid Interf. Sci. 277 (2004) 257–263.
[27] Y.S. Ho, G. McKay, Pseudo-second-order model for sorption processes, Proc. Biochem. 34 (1999) 451–465.
[28] A.S. Özcan, A. Özcan, Adsorption of acid dyes from aqueous solutions onto acid-activated bentonite, J. Colloid Interf. Sci. 276 (2004) 39–46.
[29] H. Nollet, M. Roels, P. Lutgen, P. Van der Meeren, W. Verstraete, Removal of PCBs from wastewater using fly ash, Chemosphere 53 (6) (2003) 655–665.
[30] Y. Yu, Y.Y. Zhuang, Z.H. Wang, Adsorption of water-soluble dye onto functionalized resin, J. Colloid Interf. Sci. 242 (2) (2001) 288–293.